Heliyon 10 (2024) e34116

Contents lists available at ScienceDirect

Heliyon

journal homepage: www.cell.com/heliyon

Research article

Spatial and temporal evolution characteristics and factors of heat vulnerability in the Pearl River Delta urban agglomeration from 2001 to 2022

Jiangbo Wang [a,1], Yishu Li [a], Wei Liu [b], Aiping Gou [c,*,2]

[a] College of Architecture, Nanjing Tech University, Nanjing, 211816, China
[b] Jiangsu Provincial Planning and Design Group, Nanjing, 210019, China
[c] School of Ecological Technology and Engineering, Shanghai Institute of Technology, Shanghai, 201418, China

ARTICLE INFO

Keywords:
Heat vulnerability
Spatiotemporal evolution
Influencing factors
Kernel density estimation
GTWR model

ABSTRACT

To explore the spatiotemporal evolution characteristics of heat vulnerability in the Pearl River Delta urban agglomeration during heatwave disasters, this research employs the Entropy Weight Method (EWM) to calculate the heat vulnerability assessment results for nine cities in the region spanning from 2001 to 2022. Through the application of kernel density estimation, Moran's I, and the Geographically and Temporally Weighted Regression (GTWR) model, which is proven to be superior to traditional model such as OLS, this study analyzes the dynamic distribution patterns of heat vulnerability in the study area and dissect the trends of influencing factors. The results reveal that from 2001 to 2022, the overall heat vulnerability index in the study area demonstrates a fluctuating downward trend. Key contributors to heat vulnerability include high-frequency and long-duration heatwaves, population sensitivity, and changes in residents' consumption levels. Throughout this period of development, the disparity in heat vulnerability among cities has gradually widened, indicating an overall pattern of uneven development in the region. Future attention should be focused on formulating heat adaptation strategies in areas with high vulnerability to enhance the overall sustainability of the study area.

1. Introduction

Under the influence of climate change, there has been a significant increase globally in the frequency, intensity, and duration of extreme heat events or heatwaves [1,2]. The Intergovernmental Panel on Climate Change (IPCC) Sixth Assessment Report highlighted that global warming is projected to reach 1.5 °C within the period from 2021 to 2040 [3]. Heat disasters have had significant impacts on human health, ecosystems, the economy, agriculture, energy, and water resources [4,5]. The 2003 heatwave in France, for instance, led to the tragic death of over 15,000 people [6]. In 2006, the heatwave in California resulted in approximately 1200 hospitalizations and prompted 16,000 people to seek emergency room treatment [7]. In the summer of 2010, a heatwave caused over 600 wildfires in western Russia, releasing toxic gases [8]. Three heatwave events occurring between 2011 and 2013 resulted in economic damages of

* Corresponding author.
E-mail address: gouaiping@sit.edu.cn (A. Gou).
[1] First author's introduction: Wang Jiangbo (1976), male, professor, mainly engaged in urban disaster prevention, resilient city research. E-mail: wjb623@163.com
[2] Gou Aiping (1971) female, professor, mainly engaged in eco-city, resilient city research

https://doi.org/10.1016/j.heliyon.2024.e34116
Received 26 March 2024; Received in revised form 2 July 2024; Accepted 3 July 2024
Available online 4 July 2024

approximately $60 billion in the USA [9]. The recent heatwave event in the North American region in 2022 caused at least 486 sudden deaths in the Canadian province of British Columbia within five days in June, a figure three times higher than historical records [10]. Meanwhile, the heatwave in China caused economic losses of $7.6 billion, accompanied by numerous issues such as frequent fires, dried-up rivers, suspended shipping, and power shortages [11].

In China, there is a spatial pattern of heatwave frequency and cumulative days, generally characterized by a distribution of "high in the south and low in the north" [12]. Over the past 42 years, the mortality burden caused by heatwaves has exhibited a non-linear, rapid growth in temporal evolution [13], with a more significant impact observed in the eastern and central regions. In the summer of 2022, Shanghai, Zhejiang Province, Fujian Province, and Guangdong Province have experienced the most intense heatwave since 1961 [14]. Furthermore, Chongqing witnessed more than twenty consecutive days with the daily maximum temperature exceeding 40 °C [15].

Heat and heatwaves in the Pearl River Delta have led to a range of challenges, including reduced crop yields, reservoir drying [16], insufficient drinking water supply, power shortages, and an increase in heat-related illnesses [17–19]. In 2004, drought, reduced rainfall, and prolonged high temperatures caused high forest fire risk, while on July 7, 2014, Guangdong's power grid load peaked at 90,214 million kilowatt-hours, the first in China to exceed 90 million under centralized dispatching [20]. The summer heat accelerated epidemic spread [21], with southern Guangdong, a dengue fever hotspot, reporting 45,189 cases in 2014, 90.51 % of which were in Guangzhou and Foshan [22]. In 2021, heatwaves caused the Xinfengjiang Reservoir, a key water source for the Pearl River Delta urban agglomeration, to drop to historic lows, challenging water supply security in the Dongjiang River Basin [23].

The research perspective on heatwave disasters has evolved from the traditional "disaster-risk" framework to the more comprehensive "human-environment system vulnerability" framework [24]. Initially drawing attention from meteorologists and medical scholars, the focus was on understanding patterns of heat stress and its impacts on human and environmental health [25]. In the future, it is anticipated that heatwaves will become more frequent and more intense [26]. With the involvement of scholars in geography and sociology, many researchers have adopted the Heat Vulnerability Index (HVI) to quantify the impact of heat disasters, differentiating spatially at national or city levels [27–30]. This approach assessed the sensitivity and adaptive capacity of social, economic, and environmental systems to heat risk. The HVI effectively characterizes regional vulnerability features and differences in vulnerability levels, enabling the formulation of targeted strategies [31].

However, determining heat vulnerability involves considering a multitude of factors, and there is no universally accepted set of criteria for assessing heat vulnerability [27]. The number of factors used in studies on heat vulnerability varies, ranging from 4 to 19, with selected indicators encompassing hazard exposure factors to elements related to population characteristics, socioeconomic conditions, and the built environment [32]. For instance, Cutter et al. proposed and developed the Social Vulnerability Index, listing population, environmental and social factors, including demographic characteristics like age, gender, and race, vulnerable populations with special needs, quality of human settlements, and characteristics of the built environment [33]. Numerous studies have built upon and refined Cutter's research [29]. Various methodologies, including principal component analysis and composite indices, are commonly employed to extract vulnerability factors or compute the HVI [28]. Subsequently, these indices are visualized spatially, creating maps that reveal vulnerability patterns and social disparities in extreme heat [34,35]. Some scholars utilized remote sensing techniques to identify extreme heat and employ the Principal Component Analysis (PCA) or the Entropy Weight Method (EWM) to explore the spatial distribution of the HVI. Researches have shown that city centers often tend to exhibit higher vulnerability aggregation [36,37]. The study of heat vulnerability spanned a broad range of scales, from focusing on communities [38] to national scales [39]. Indeed, not confined to disaster-prone regions, HVI calculations have also been extended to cold regions [40].

The vulnerability concept framework of Exposure-Sensitivity-Adaptive Capacity (ESA) has been widely applied in the vulnerability assessment of heat disasters [35,41–43]. This framework, encompassing vulnerability assessments of various components within the system, has provided a comprehensive understanding of the potential risk levels the system may face under different scenarios. Exposure reflects the characteristics, intensity, frequency, or degree of danger that a complex system in a given region faces from heat risk. Sensitivity refers to the degree of change in the internal structure and functions of the system under the stress of heat, contingent on the stability of the system. Adaptive capacity [24] refers to the system's ability to responds disaster events, as well as its ability to recover from disaster losses, reflecting the degree to which the system can mitigate and reduce the damage from disasters.

At the same time, as comprehensive research into vulnerability drivers and evolutionary mechanisms gradually deepens, regression analysis methods have been widely used in studies related to disaster vulnerability, such as traditional OLS regression [44,45], Geographically Weighted Regression (GWR) [46], Multiscale Geographically Weighted Regression(MGWR) [47], and Spatial Autoregressive Models (SAM) [48]. Although models like GWR can effectively capture spatial heterogeneity, they do not inherently account for temporal dynamics [49], which are crucial for the evolution of heat vulnerability. The Geographically and Temporally Weighted Regression (GTWR) model, a variant of the GWR model, can incorporate spatial and temporal information into the weighting matrix, thus identifying spatiotemporal heterogeneity. This model is currently gaining attention in research on spatiotemporal [50].

In general, vulnerability is dynamic [51–53]. On one hand, the intensity of heatwave disasters consistently surpasses thresholds, and the environmental and socio-economic context influencing vulnerability is continually changing. However, existing studies on heat vulnerability are primarily constrained by surface temperature data [54] and rely on cross-sectional data with large time spans [55,56]. There is still room for exploration in establishing a heat vulnerability framework that integrates a complete understanding of the dynamic process of heatwaves. On the other hand, existing research predominantly focuses on the selection of heat vulnerability indicators [28], framework construction [57], and vulnerability distribution patterns [58,59], with less attention to the spatiotemporal evolution and underlying causes of vulnerability. Simultaneously, the study area exhibits imbalances in climate change and socio-economic development, which may lead to significant variations in heat vulnerability at the spatial or regional level [60] that has received relatively less research attention.

Therefore, this study extends existing research by constructing a heat vulnerability assessment framework and indicator system from the dimensions of exposure, sensitivity, and adaptive capacity. This research utilizes the EWM and addition-subtraction method [61] to calculate multi-year heat vulnerability assessment results. Additionally, methods such as Kernel density estimation and Geographically and Temporally Weighted Regression(GTWR) model [62] have been employed to identify the spatiotemporal evolution characteristics and influencing factors of heat vulnerability at the regional scale of the study area from 2001 to 2022.

This study is the first to conduct a continuous dynamic analysis of heat vulnerability specifically for the Pearl River Delta urban agglomeration, enriching the indicator framework and offering higher temporal resolution compared to previous research. Meanwhile, methodologically, it innovatively employs the GTWR model, which has a higher robust goodness-of-fit, for investigating the causes of heat vulnerability, fully accounting for temporal and spatial non-stationarity.

The aim of this research is to comprehensively illustrate the spatiotemporal dynamic development trends of heat vulnerability in the Pearl River Delta urban agglomeration, elucidate the characteristics of heat disasters, and explore more response information of the study region. The research intends to provide a theoretical reference to promote the establishment of a climate community of shared destiny in the study area and support regional coordinated development.

2. Data and methodology

2.1. Overview of the study area

This study focuses on the urban agglomeration comprising Guangzhou, Shenzhen, Foshan, Dongguan, Zhongshan, Zhuhai, Huizhou, Jiangmen, and Zhaoqing in the Pearl River Delta (Fig. 1), which is chosen as the primary research area due to its high level of urbanization and close economic ties. Covering a total area of 54,766,62 square kilometers, it represents only 0.52 % of the national territory but is home to 5.55 % of the whole country's population. Moreover, in 2022, its GDP accounted for 8.65 % of the national total [63,64].

The majority of the region is located south of the Tropic of Cancer, featuring diverse topography that includes plains in the central part, as well as mountainous areas, hills, and islands. Influenced by both continental monsoons and maritime monsoons, the climate in this region is complex and variable. Simultaneously, global warming and rapid urbanization have garnered significant attention, particularly in relation to heat-related environmental issues [65].

As of the 7th National Population Census in 2021, the population in the study area has increased from 561, 18 million in 2010 to 780, 14 million in 2020, reflecting a growth of 39 %, and this upward trend is expected to continue. In 2022, the overall climate in the region was characterized by a high number of hot days with strong intensity [66]. As a result, against the backdrop of climate change

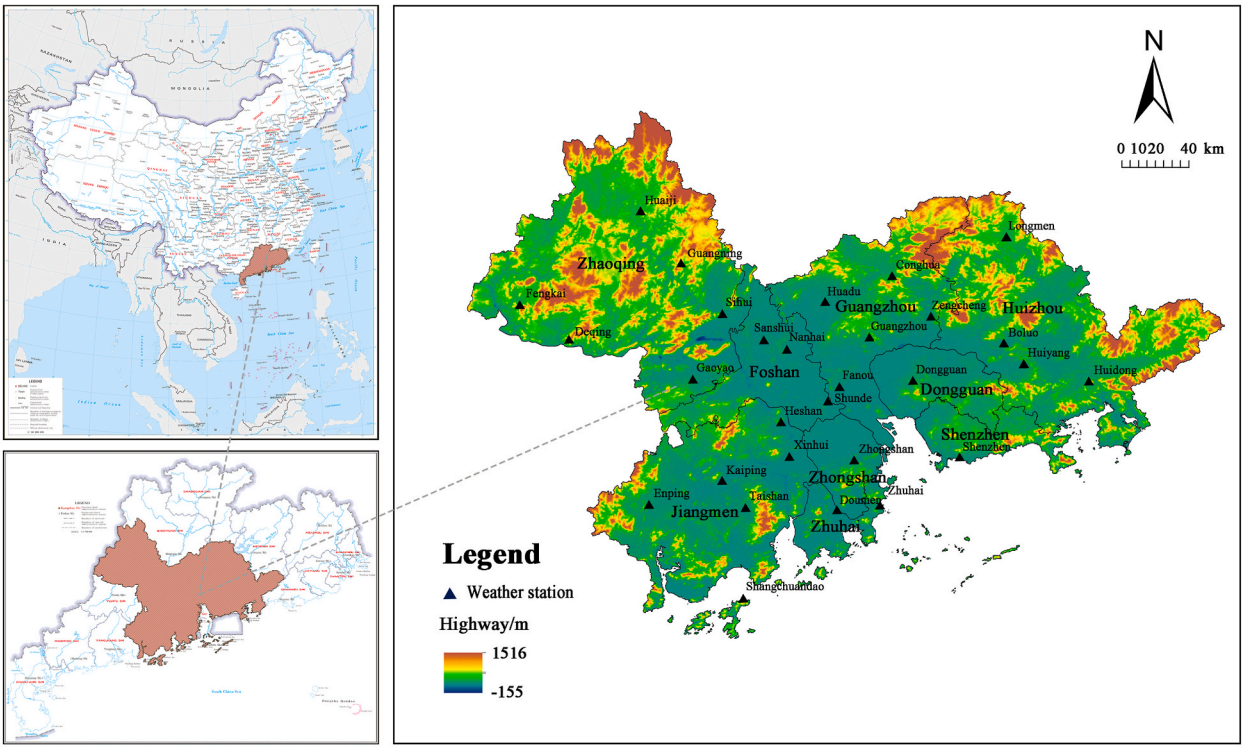

Fig. 1. Geographic Location of the study area.
[Image Source: Map drawn by the author based on Survey Numbers GS(2022)4314 and Yue S(2022)315]

and rapid population growth, the study area is expected to face severe challenges related to water resource security, as well as significant pressure for disaster prevention, reduction, and relief efforts [67,68].

2.2. Data sources

This study adopts the criteria established by the China Meteorological Administration regarding high-temperature weather and heatwaves. It categorizes days with daily maximum temperatures ≥35 °C as high-temperature days [43]. When such high-temperature conditions persist for three or more consecutive days, it is identified as a heatwave [31].

29 national meteorological stations have been chosen within the study area from 2001 to 2022 (Fig. 1). Utilizing python and ordinary kriging spatial interpolation based on the latitude and longitude of meteorological stations, the study generated daily 0.1° raster maps of maximum temperatures (Table 1). By combining administrative boundary data of prefecture-level cities in China with temperature raster maps, the study calculated the daily average maximum temperature values for prefecture-level cities within the study area.

2.3. Methods

2.3.1. Construction of the heat vulnerability framework

The risk of heat disasters is jointly determined by the exposure, sensitivity, and adaptive capacity of the vulnerable system. Drawing upon previous studies [69,70], the study selected 19 specific, feasible, and scientifically sound quantitative indicators from these three dimensions, to assess the heat vulnerability of spatial units in study area (Table 2). Indicators related to heatwaves have been included in the framework. In addition, the study further subdivided the sensitivity and adaptive capacity dimensions into environmental, economic and social dimensions, in order to assess the vulnerability in all aspects.

First of all, non-dimensional standardization is performed on positive indicators (larger values are better) and negative indicators (smaller values are better) based on the extreme value method.

Positive indicators:

$$x'_{ij} = \frac{x_{ij} - \min\{x_{1j}, \ldots, x_{nj}\}}{\max\{x_{1j}, \ldots, x_{nj}\} - \min\{x_{1j}, \ldots, x_{nj}\}} \tag{1}$$

Negative indicators:

$$x'_{ij} = \frac{\max\{x_{1j}, \ldots, x_{nj}\} - x_{ij}}{\max\{x_{1j}, \ldots, x_{nj}\} - \min\{x_{1j}, \ldots, x_{nj}\}} \tag{2}$$

Where x_{ij} represents the value of the j-th indicator for the i-th city (i = 1, 2, …, n. j = 1, 2, …, m). The normalized value is denoted as x'_{ij}, but for convenience, the normalized data in the following calculations is still represented as x_{ij}. In the establishment of the comprehensive model for vulnerability assessment indicators, the weights of various dimension indicators are determined using the EWM [83] to avoid the subjective impact of assigning weights. The mathematical expressions of the entropy method are as follows:

Calculate the proportion of the i-th city for the j-th indicator:

$$p_{ij} = \frac{x_{ij}}{\sum_{i=1}^{n} x_{ij}} \tag{3}$$

Calculate the entropy value for the j-th indicator:

$$e_j = -k \sum_{i=1}^{n} p_{ij} \ln p_{ij} \tag{4}$$

Table 1
Sources of research data.

Data Name	Date	Resolution	Source
Administrative boundary data	2022	/	Institute of Geographic Sciences and Natural Resources Research, Chinese Academy of Sciences (https://www.resdc.cn/)
Daily maximum temperature data	2001–2022	Daily	China Surface Climate Daily Value Dataset V3 (https://data.cma.cn/)
Socioeconomic data	2001–2022	Annually	China Statistical Yearbook, China Urban and Rural Statistical Yearbook, Guangdong Statistical Yearbook, Statistical Yearbooks of 9 prefecture-level cities, National Economic and Social Development Statistical Bulletin
Population quantity and structure data	2000, 2010, 2020	Annually	the Fifth, Sixth, and Seventh National Population Censuses
Water resource data	2001–2022	Annually	Guangdong Provincial Water Resources Bulletin
NDVI data	2001–2022	Annually	NASA MOD13A3 Dataset (https://search.earthdata.nasa.gov/search)

Table 2
Framework for heat vulnerability assessment in study area.

Measurement System for Heat Vulnerability	Target layer	Dimension Layer	Indicator layer	Definition of Indicators	Unit (of measure)	Weights	References
	Heat Exposure	Exposure	Average annual maximum temperature	Annual maximum mean temperature	°C (+)	0.206	[71]
			High temperature days	Number of days with daily maximum temperature greater than or equal to 35 °C	Day (+)	0.165	[31,69]
			Heatwave frequency	Number of heatwave events	Times (+)	0.162	[27,31]
			Duration of heatwaves	Total duration of heatwave events	Day (+)	0.150	[31]
			Intensity of heatwaves	Cumulative temperature above 35 °C during heatwave events	°C(+)	0.149	[27,31]
			Permanent resident population	Population Exposed to heat risk	Ten thousand (+)	0.168	[31]
	Heat Sensitivity	Environmental Sensitivity	Population density	Spatial distribution aggregation of population	Person per square kilometers (+)	0.055	[37,41,72]
			Water resources emergency capacity	Total water resources	Billion cubic meters per year (−)	0.151	[73,74]
		Economic Sensitivity	Local fiscal general public budget expenditure	Public financial expenditure	a hundred million (−)	0.176	[72]
			Regional gross domestic product (GDP)	Economic level	a hundred million (−)	0.172	[31]
			Consumer price index	Resident consumption power	% (−)	0.116	[74]
		Social Sensitivity	Proportion of female population	Reflects the vulnerability characteristics of the female	% (+)	0.126	[43,75]
			Proportion of population aged 0-14	Reflects the vulnerability characteristics of the children	% (+)	0.098	[76]
			Proportion of population over 65 years old	Reflects the vulnerability characteristics of the elderly	%(+)	0.105	[37, 77–79]
	Heat Adaptive Capacity	Social Factors	Number of health institutions	Alternative indicators for the level of health protection against heatwave disasters	(−)	0.212	[43,80,81]
			Number of beds in health institutions	Alternative indicators for the level of health protection against heatwave disasters	(−)	0.171	[81]
			Number of health technical personnel	Alternative indicators for the level of health protection against heatwave disasters	Person (−)	0.161	[43,81]
		Economic Factors	Gross domestic product (GDP) per capita	Availability of Cooling Facilities in Household	Yuan (−)	0.231	[43,79]
		Environmental Factors	Normalized Difference Vegetation Index (NDVI)	Greening Level for Coping with High Temperatures	(−)	0.224	[31,35,82]

In the formula: $k = \frac{1}{\ln n}$, $e_j \geq 0$.

Calculate the redundancy of information entropy for the j-th indicator:

$$d_j = 1 - e_j \tag{5}$$

Calculate the weights for each indicator :

$$w_j = \frac{d_j}{\sum_{j=1}^{m} d_j} \tag{6}$$

In this study, HVI is calculated using the addition and subtraction method. The indices for each dimension layer are computed using the weighted summation method, which effectively reflects the synergistic relationship among the three dimensions. Mathematical expressions are as follows:

$$\mathrm{HVI} = \mathrm{EI} + \mathrm{SI} \ - \ \mathrm{AI} \tag{7}$$

$$EI = \sum_{j=1}^{m} w_{ij} * p_{ij} \tag{8}$$

$$SI = \sum_{j=1}^{m} w_{ij} * p_{ij} \tag{9}$$

$$AI = \sum_{j=1}^{m} w_{ij} * p_{ij} \tag{10}$$

In the model HVI represents the Heat Vulnerability Index. EI, SI, AI represent the Exposure Index, Sensitivity Index, and Adaptive Capacity Index, respectively. w_{ij} denotes the weight of the j-th indicator for the i-th region (refer to Table 2), and p_{ij} represents the standardized value of the j-th indicator for the i-th region.

2.3.2. Kernel density estimation

Kernel density estimation is capable of estimating the probability density of a random variable. It uses a continuous density curve and employs smoothing methods to describe the distribution pattern of the random variable, thereby investigating whether a uniform distribution phenomenon exists [84,85]. In this study, the Kernel density estimation method is employed to illustrate the distribution pattern of the HVI of the study area. Mathematical expressions are as follows:

$$f(x) = \frac{1}{N\not{h}} \sum_{i=1}^{N} K\left(\frac{x_i - \overline{x}}{\not{h}}\right) \tag{11}$$

$$K(x) = \frac{1}{\sqrt{2\pi}} \exp\left(-\frac{x^2}{2}\right) \tag{12}$$

Where x is the random variable. N is the number of regional prefecture-level cities. x_i represents the comprehensive index of the i-th city. $\overline{x}$ represents the average of the comprehensive index. K (·) represents the Kernel density, and h represents the window width, determining the precision in the kernel density estimation.

MATLAB 2022b software has been utilized to run the Kernel density model, dynamically estimating all time points during the research period. Through comparisons at different time periods, this study aims to form a comprehensive understanding of the HVI of the study area, and capture the overall morphology and dynamic characteristics of its evolution.

2.3.3. Exploratory spatial data analysis

The Moran Index is divided into the Global Moran Index and the Local Moran Index [86], both of which are used to measure the overall clustering tendency and the clustering tendency between cities in the study area, respectively.

$$I_G = \frac{\sum_{a=1}^{n} \sum_{b=1}^{n} w_{ab}(x_a - \overline{x})(x_b - \overline{x})}{S^2 \sum_{a=1}^{n} \sum_{b=1}^{n} w_{ab}} \tag{13}$$

$$I_L = \frac{x_a - \overline{x}}{S^2} \sum_{b=1}^{n} w_{ab}(x_a - \overline{x}) \tag{14}$$

In the formula the I_G represents the Global Moran Index, and the I_L represents the Local Moran Index. The x_a and the x_b are the HVI of regions a and b, respectively. The $\overline{x}$ is the average of the HVI. The S^2 is the variance of the HVI, and the w_{ab} is an element in the spatial weight matrix.

If $I_L > 0$, it indicates a positive spatial correlation among the HVI of various cities in the study area, meaning that the study objects are clustered spatially. While if $I_L < 0$, it indicates a negative spatial correlation among the HVI of various cities in the study area, meaning that the study objects are dispersed spatially. If $I_L = 0$, it suggests a random distribution of the study objects.

2.3.4. Geographically and Temporally Weighted Regression (GTWR) model

The GTWR model introduces a temporal dimension on the basis of the Geographically Weighted Regression (GWR) model [87]. Utilizing panel data for spatial regression, this model effectively takes into account both temporal and spatial non-stationarity [88], enhancing the accuracy of estimation results. The model is expressed as follows:

$$Y_i = \beta_0(u_i, v_i, t_i) + \sum_{k=1}^{p} \beta_k(u_i, v_i, t_i) X_{ik} + \varepsilon_i \quad (15)$$

In the model, the variables u_i and v_i represent the latitude and longitude coordinates of the gravity center of each city, and (u_i, v_i, t_i) denote the spatiotemporal coordinates of the ith city. X and Y refer to the explanatory and dependent variables, respectively, with p representing the number of explanatory variables. $\beta_0(u_i, v_i, t_i)$ is the intercept term, and $\beta_k(u_i, v_i, t_i)$ is the estimated coefficient for the kth explanatory variable. ε_i represents the model residuals.

To eliminate multicollinearity among the data, a Variance Inflation Factor (VIF) test is conducted for each indicator, where $0 < VIF < 10$ indicates the absence of multicollinearity. In this study, a total of 12 indicators have been ultimately selected for analysis (Table 3).

3. Results and analysis

3.1. The evolutionary characteristics over time dimension

3.1.1. The overall HVI decreases over time

The overall HVI in the study area showed a decreasing trend over the period from 2001 to 2022 (Fig. 2). The density function curve shifted towards lower values, with a noticeable shift towards higher values in 2004. This may be related to the heatwave at the end of June to early July in 2004, which led to 39 deaths from heatstroke in Guangzhou [89], multiple car fires, and peak water and electricity consumption throughout the city.

The density function curve of the heat exposure index showed a trend of shifting towards higher values over time, with an overall transition from a single-peak to a multi-peak shape. This indicates an increasing danger due to frequent extreme heatwave events and rapid population concentration exposed to heat risk.

The density function curve of the heat sensitivity index was mainly characterized by a M-shaped bimodal distribution, suggesting complexity in the disaster situation within the study area, with variations in the sensitivity level. The highest peaks were concentrated in the high-value region, indicating a trend of initially decreasing and then increasing over time. After 2020, the density curve of heat sensitivity showed an increasing trend, reflecting the need for the study area to enhance adaptation measures to reduce its own sensitivity.

The density function curve of the heat adaptation capacity index showed a slight and steady shift over time, presenting an increasing trend. The maximum peak value of the density function curve changed relatively little over the sample period, with the mode of heat adaptation capacity concentrated between 0.3 and 0.4. The overall shape of the curve transitioned from a single-peak to a multi-peak pattern, gradually exhibiting more pronounced skewed multi-modal distribution characteristics, with peaks aggregating towards higher numerical values. The overall adaptation capacity of the study area to heat risk showed stable development over time, while vulnerable areas exhibited extreme sensitivity to heat disasters. Due to factors such as the lagging resilience development in the face of heatwave compared to economic growth, these areas may find it challenging to reach the average level in a short period.

3.1.2. The HVI in the majority of cities shows a declining trend

The majority of cities in the Pearl River Delta urban agglomeration showed decreasing values of the HVI over time (Fig. 3). Based on the growth rate at the end compared to the beginning of the period, the cities can be categorized into three types: ① Rapid decline with significant fluctuations (decrease >50 %), including Guangzhou and Shenzhen. ② Slow decline with Fluctuations (0 % < decrease ≤50 %), including Foshan, Huizhou, Zhaoqing, Dongguan, Zhuhai, and Jiangmen. ③ Fluctuating increase (decrease ≤0), represented by Zhongshan, which is primarily due to its significantly higher sensitivity to high temperature days compared to other cities.

Table 3
Indicators selected by GTWR model.

Target Layer	Variable Name	Unit (of measure)	VIF
Heat Exposure	Average annual maximum temperature	°C	1.793
	High temperature days	Day	4.723
	Heatwave frequency	Times	4.334
Heat Sensitivity	Population density	Person per square kilometers	4.028
	Water resources emergency capacity	Billion cubic meters per year	5.584
	Consumer price index	%	1.312
	Proportion of female population	%	1.561
	Proportion of population aged 0-14	%	2.586
	Proportion of population over 65 years old	%	5.586
Heat Sensitivity	Number of health institutions	/	7.123
	Number of beds in health institutions	/	5.681
	GDP per capita	Yuan	3.277

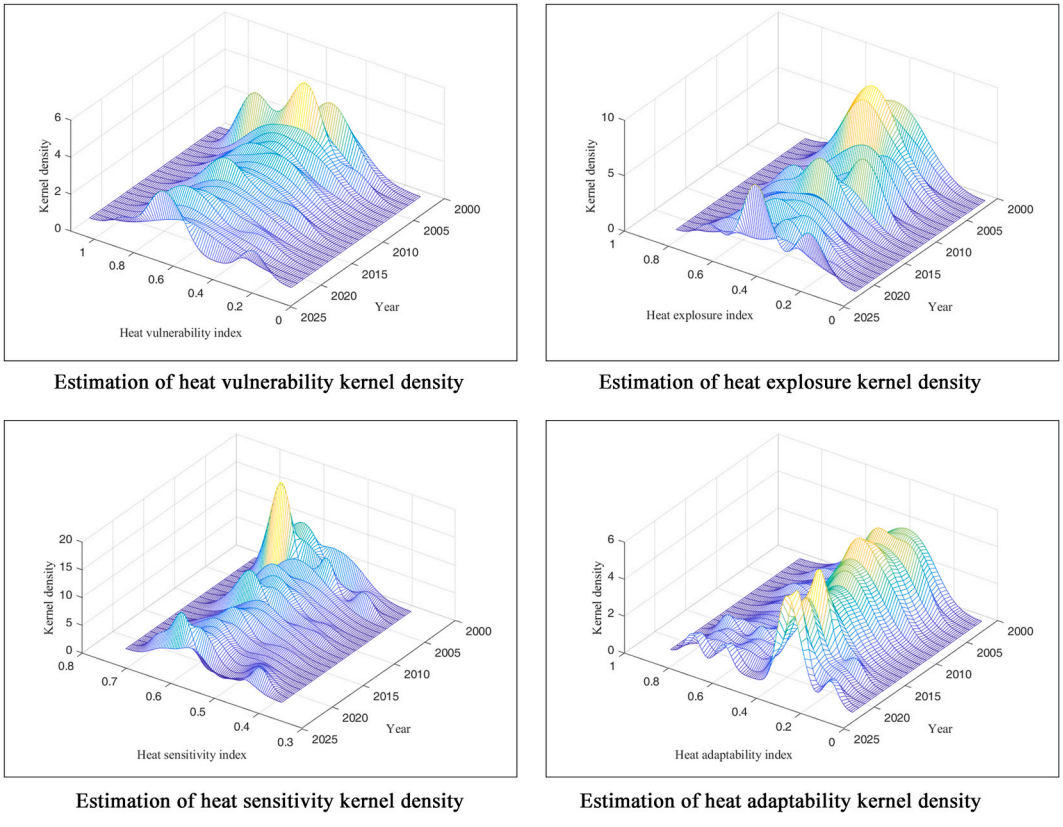

Fig. 2. The dynamic evolution of heat vulnerability and various dimension indices in the study area from 2001 to 2022.

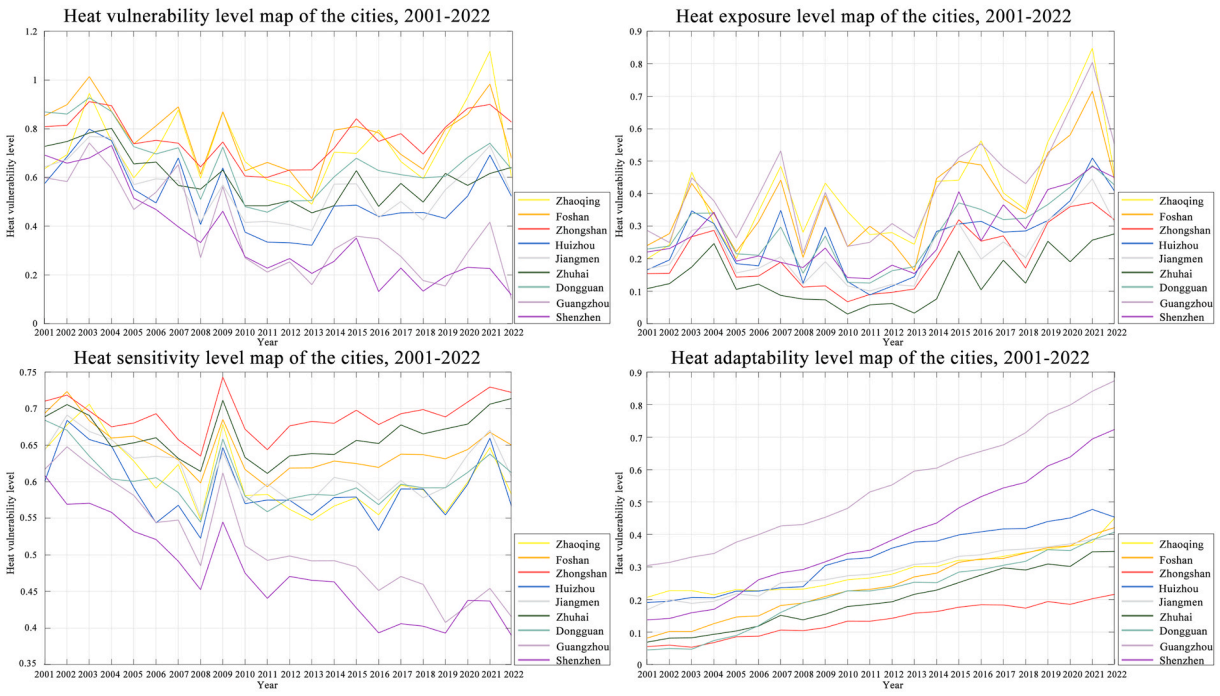

Fig. 3. Changes in Vulnerability Indices of Cities in the study area from 2001 to 2022.

The vulnerability index curves of various cities experienced intense fluctuations from 2001 to 2010, stabilized between 2010 and 2012, and showed minor fluctuations after 2012. In 2011, Guangdong Province established the country's first emergency meteorological channel, rapidly disseminating meteorological warning information and emergency science popularization knowledge [20]. In addition to the decreasing threat of heatwave disasters in the Pearl River Delta urban agglomeration, the intensified efforts in heat prevention measures such as heat subsidies, and the shift in economic development patterns have contributed to the reduction of the HVI.

The difference in HVI among cities gradually increased over time. From 2001 to 2010, the trends among cities were similar, with relatively small differences. However, after 2010, a trend of clustered changes gradually formed. Cities like Zhaoqing, Foshan, and Zhongshan exhibited significantly higher HVI compared to other cities. Dongguan, Jiangmen, Huizhou, and Zhuhai showed a clustered trend in the changes of HVI. Meanwhile, Guangzhou and Shenzhen displayed a clustered trend of decreasing HVI. The difference of HVI between the cluster of Zhaoqing, Foshan, Zhongshan and the cluster of Guangzhou, Shenzhen gradually became more pronounced.

In the dimension of heat exposure, the heat exposure indices of various cities generally showed an increasing trend, accompanied by significant fluctuations. All regions reached the peak of the heat exposure index in 2021, and the differences in exposure between different regions gradually increased. Specifically, Zhuhai and Zhongshan maintained relatively low levels of heat exposure indices. In contrast, Zhaoqing, Guangzhou, and Foshan consistently maintained higher levels of heat exposure indices, indicating that these areas are more susceptible to the risk of exposure to heatwave disasters, consistent with previous research results [79].

In the dimension of heat sensitivity, all cities except Zhongshan and Zhuhai showed a fluctuating downward trend in the index. Among them, Guangzhou and Shenzhen exhibited a particularly significant decrease. An analysis of the trend in indicators revealed that the local fiscal general public budget expenditures in Guangzhou and Shenzhen have significantly increased, surpassing other prefecture-level cities, contributing to their relatively good performance in terms of heat sensitivity. The higher sensitivity in Zhongshan and Zhuhai was attributed to low water resource reserves and a relatively higher proportion of female population.

In the dimension of heat adaptability, the indices of all cities were steadily increasing year by year. The rate of increase in heat adaptability in Guangzhou was significantly higher than in other cities, and Shenzhen has rapidly risen to become the second-ranked city in the adaptability index from a low value at the beginning of the time range. Due to its geographical and economic advantages, the study area has abundant clinical resources and human resources, leading in "Interne and healthcare" and showing rapid momentum in technological innovation and development. However, the current level of medical development in the region is uneven. With a rapidly growing economic level, Guangzhou and Shenzhen have more comprehensive social security systems, providing better medical security and social services to cope with issues such as heatstroke caused by heatwave disasters. At the same time, the two cities had different focuses in medical development. Guangzhou tends to develop into a medical hub, radiating to improve the overall medical standards of the study area, while Shenzhen emphasizes consolidating grassroots medical care, considering health management and elderly care as growth points [90].

3.2. The evolutionary characteristics in spatial dimension

3.2.1. The transition from negative correlation to positive correlation in space

Due to the polarization phenomenon of HVI within the study area from 2001 to 2022 (Fig. 3), temporal analysis alone cannot determine the clustering degree and mutual influence of HVI in spatial dimension. Therefore, this section will explore the spatial

Table 4
Global Moran's index and tests.

Year	Moran's I	p	z
2001	−0.584	0.018	−1.820
2002	−0.652	0.005	−2.165
2003	−0.127	0.472	−0.009
2004	−0.571	0.012	−1.886
2005	−0.504	0.044	−1.507
2006	0.037	0.261	0.631
2007	0.140	0.171	1.093
2008	−0.089	0.416	0.123
2009	0.069	0.214	0.755
2010	0.114	0.190	0.894
2011	0.094	0.204	0.820
2012	0.031	0.336	0.345
2013	−0.226	0.386	−0.414
2014	−0.036	0.338	0.345
2015	−0.130	0.461	−0.030
2016	−0.012	0.333	0.388
2017	−0.136	0.474	−0.054
2018	−0.319	0.233	−0.787
2019	−0.006	0.291	0.449
2020	0.015	0.271	0.543
2021	0.085	0.211	0.848
2022	−0.264	0.330	−0.595

distribution of HVI in the study area.

The results of global spatial autocorrelation analysis (Table 4) showed that from 2001 to 2004, there was a significant negative spatial correlation of HVI in the study area. However, after 2005, this negative spatial correlation gradually weakened and evolved towards positive correlation. This phenomenon indicated that some common influencing factors are gradually shared within the region, leading to the relative clustering of high-vulnerability areas.

Taking the years 2001, 2004, 2007, 2010, 2013, 2016, 2019, and the year with the high outbreak of heatwave events in 2021, as well as 2022, as examples for local spatial autocorrelation tests. During the sample period, the study area gradually exhibited a high-high agglomeration effect (Fig. 4). Overall, cities did not exhibit significant local spatial autocorrelation during the study period, except Dongguan, Jiangmen, and Huizhou.

Notably, Jiangmen experienced a shift from low-high value areas in 2004–2013 to high-high value areas in 2019. This transition likely reflected the combined effects of climate change and environmental factors within the region, leading to an increase in heat vulnerability across the entire area surrounding Jiangmen. This trend warranted widespread attention. In contrast, Dongguan consistently exhibited high-low value areas, indicating that Dongguan itself has high heat vulnerability, while the surrounding areas have relatively low heat vulnerability. This suggested that the influence of the surrounding areas on Dongguan was relatively small. Similarly, Huizhou showed a trend from low-low value areas to high-low value areas during 2019–2022, reflecting that the city has become more vulnerable to heat over this period.

Taken together, the cases of Jiangmen, Dongguan, and Huizhou underscore the varying degrees of heat vulnerability and the need for targeted strategies to address these challenges in different urban contexts.

3.2.2. The overall trend of vulnerability levels shows a decreasing tendency

To further compare the spatial pattern evolution of HVI among different spatial units within the study area, the map is categorized into three types: low vulnerability area, medium vulnerability area, and high vulnerability area, using the natural breakpoint method (Fig. 5).

During the sample period, the area of regions with medium to high levels of HVI initially increased and then decreased. In 2004, the overall level of temperature vulnerability increased, with a significant increase in the area of high vulnerability. This trend gradually showed a pattern of high vulnerability in the eastern and western regions and low vulnerability in the central region. This may be attributed to the increase in temperature and the occurrence of more extreme weather events, leading to greater heat pressure on cities. After the extreme heat in 2021, the implementation of response measured and the improvement of social adaptability led to a certain

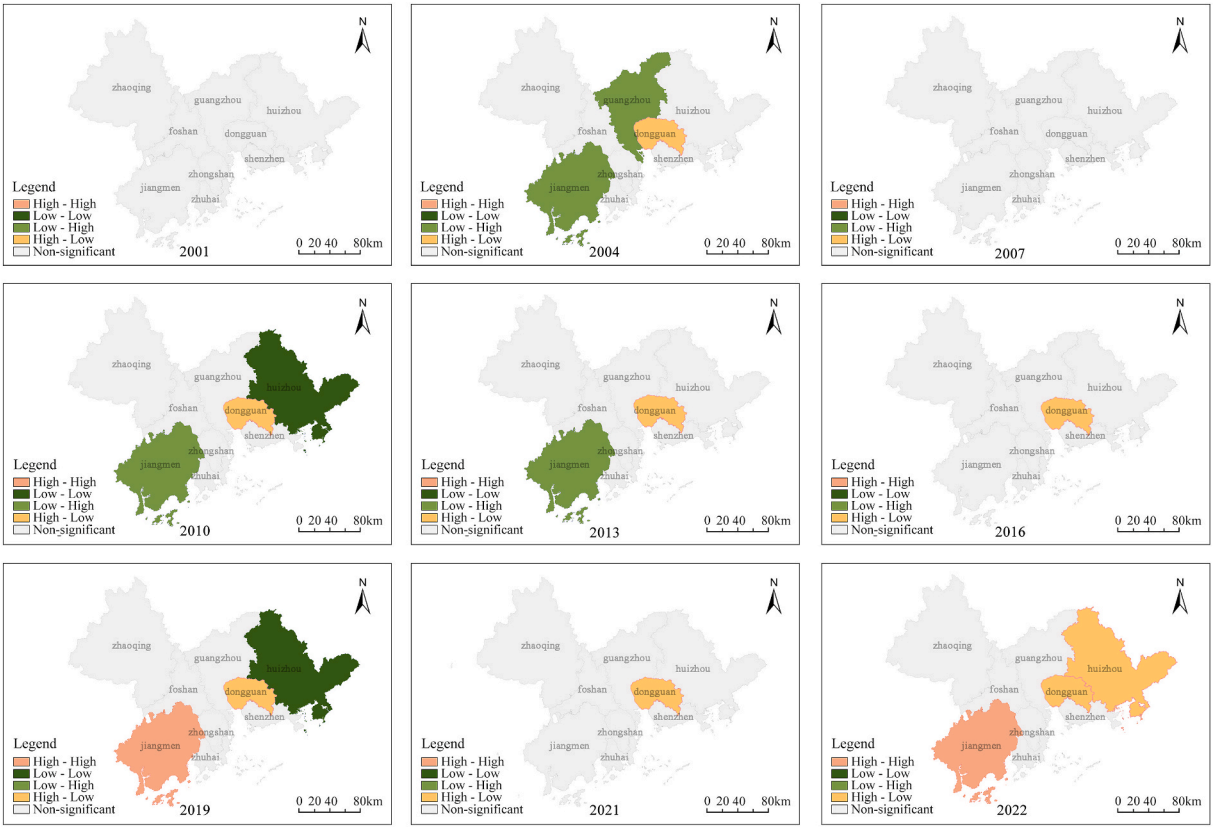

Fig. 4. Local Moran's Index of HVI in the study area from 2001 to 2022.

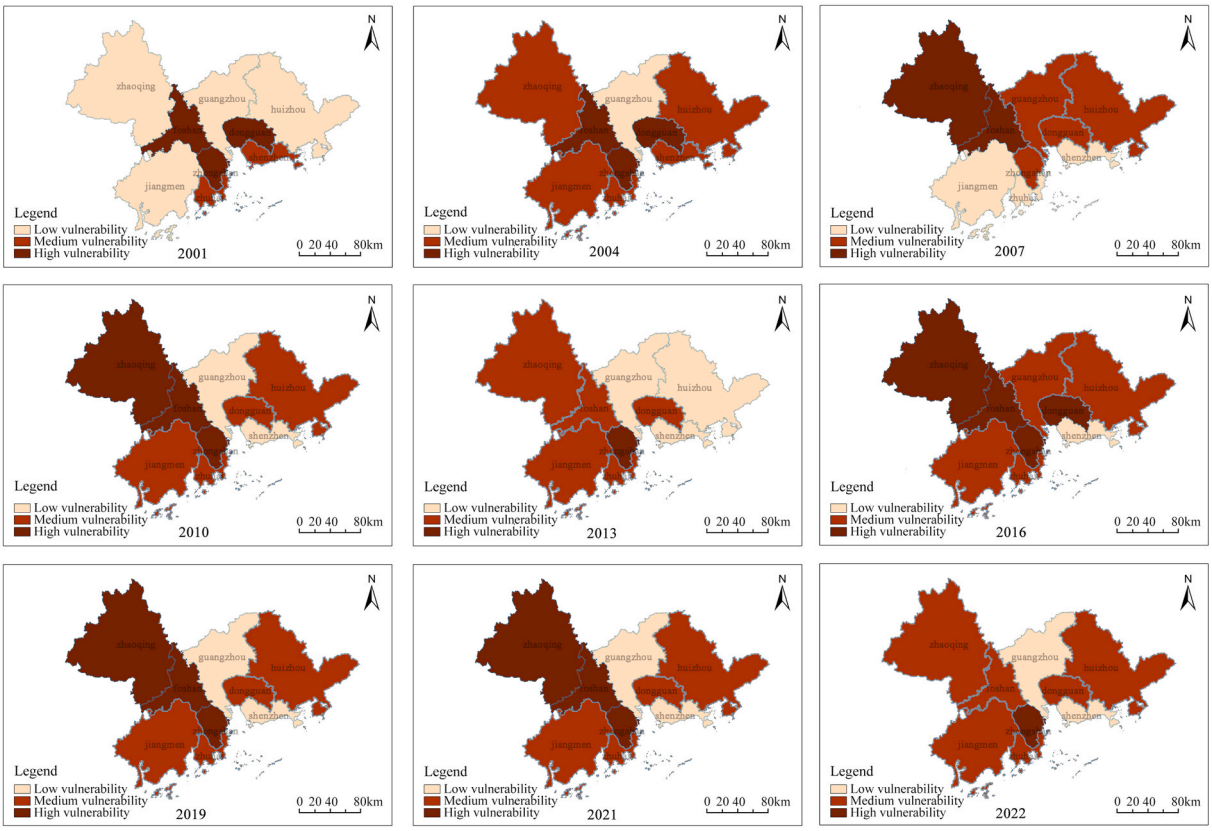

Fig. 5. Distribution of HVI for Cities in the study area from 2001 to 2022.

degree of degradation in heat vulnerability in Zhaoqing and Foshan in 2022.

Cities in medium and high vulnerability areas have evolved from a block-like distribution to a continuous pattern, such as Foshan and Zhongshan. Cities with low vulnerability have transitioned from a multi-center to a single-center pattern, as seen in Guangzhou and Shenzhen. Despite the high population density in central cities, their lower HVI was attributed to economic development and strong radiation capacity. This suggested that the level of economic development may have a strong inhibitory effect on the heat vulnerability of cities.

3.3. Analysis of influencing factors

3.3.1. Modelling evaluation

The adjusted R2 for the GTWR model is 0.86, showing an improvement of 0.02 compared to the OLS model. Also, the AICc is reduced by 92.298, indicating that the GTWR model has a higher goodness of fit and performs better in analyzing the explanatory variables (Table 5).

3.3.2. Temporal evolution volatility of influencing factors

According to the regression results of the GTWR model, the estimated coefficients of various influencing factors on the HVI of the study area were obtained at different time and space locations. Based on this, box plots have been drawn to explore their temporal evolution patterns (Fig. 6).

(1) Heat Exposure

Table 5
Comparative results of OLS and GWTR models.

Models	OLS	GTWR
AICc	−810.513	−902.811
R2	0.97896	0.99762
Adjusted R2	–	0.99747

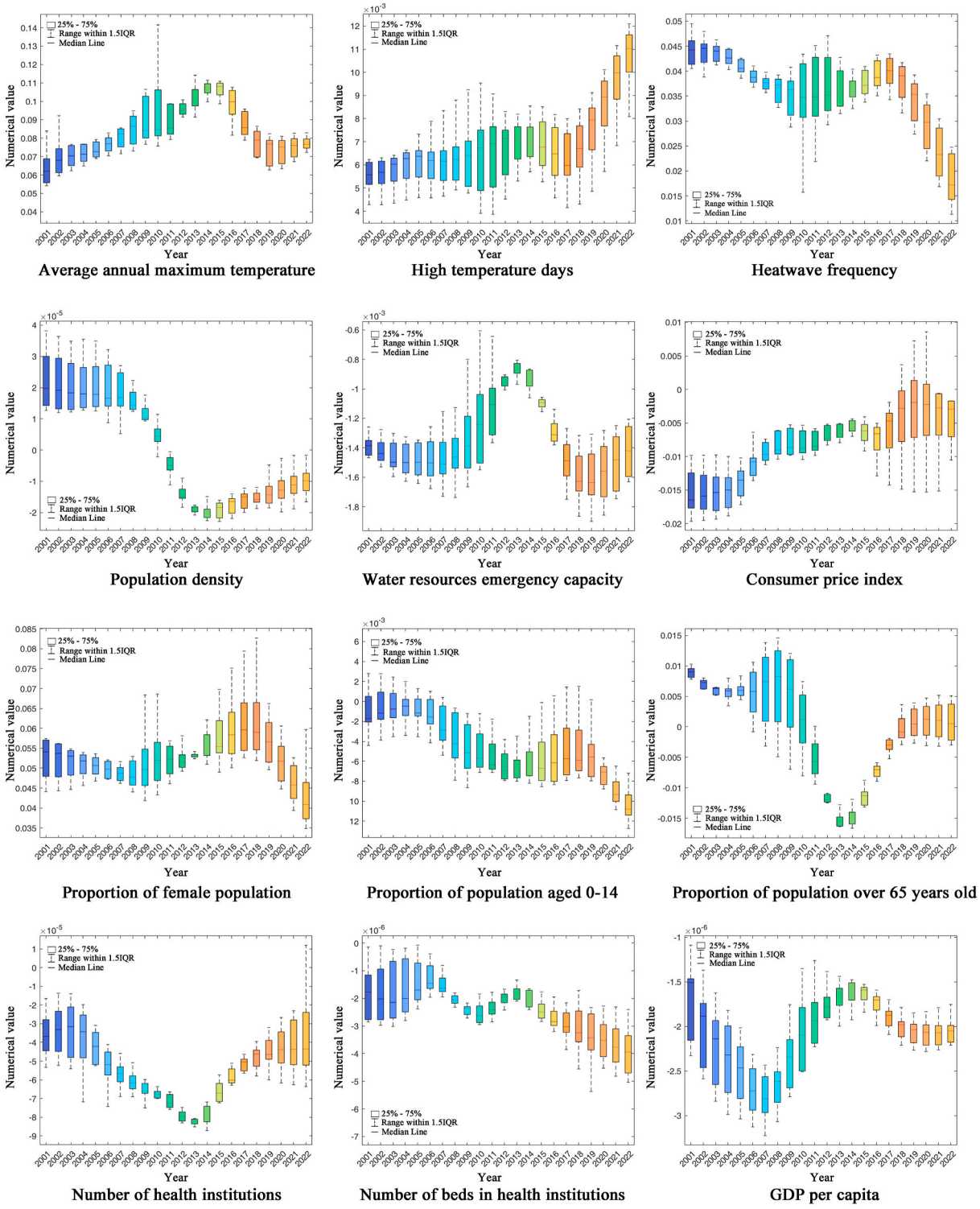

Fig. 6. Trend of changes in regression coefficients of explanatory variables from 2001 to 2022.

The main influencing indicators were the annual average maximum temperature, high temperature days and heatwave frequency, all of which had a positive effect on the HVI.

The contributions of the annual average maximum temperature and high temperature days to HVI were in a fluctuating upward trend. Therefore, it is necessary to strengthen year-round meteorological monitoring, improve the accuracy of predicting extreme

heatwave events, and ensure the rapid and effective implementation of measures during heatwave events.

(2) Heat Sensitivity

In the sensitivity dimension, the factors of the female population ratio and the consumer price index (CPI) had a relatively strong influence. Water resource emergency capacity, CPI, and the population ratio of 0–14 years old showed a negative correlation with HVI, while the female population ratio showed a positive correlation. Population density and population ratio of 65 years and above exhibited stage-wise changes.

Firstly, the population density factor had a promoting effect before 2011 and exerted an inhibitory effect after 2011, which may be due to the rapid urbanization process in the study area. The significant growth in population density in Zhongshan, Guangzhou, Foshan, Dongguan, and Shenzhen in 2009–2010 led to the concentration of the population in relatively small areas. This concentration may have resulted in a stronger urban heat island effect, making urban areas more susceptible to heat risk. Over time, the urbanization process has become more stable, and after macroeconomic regulation and control at the national and regional levels, population

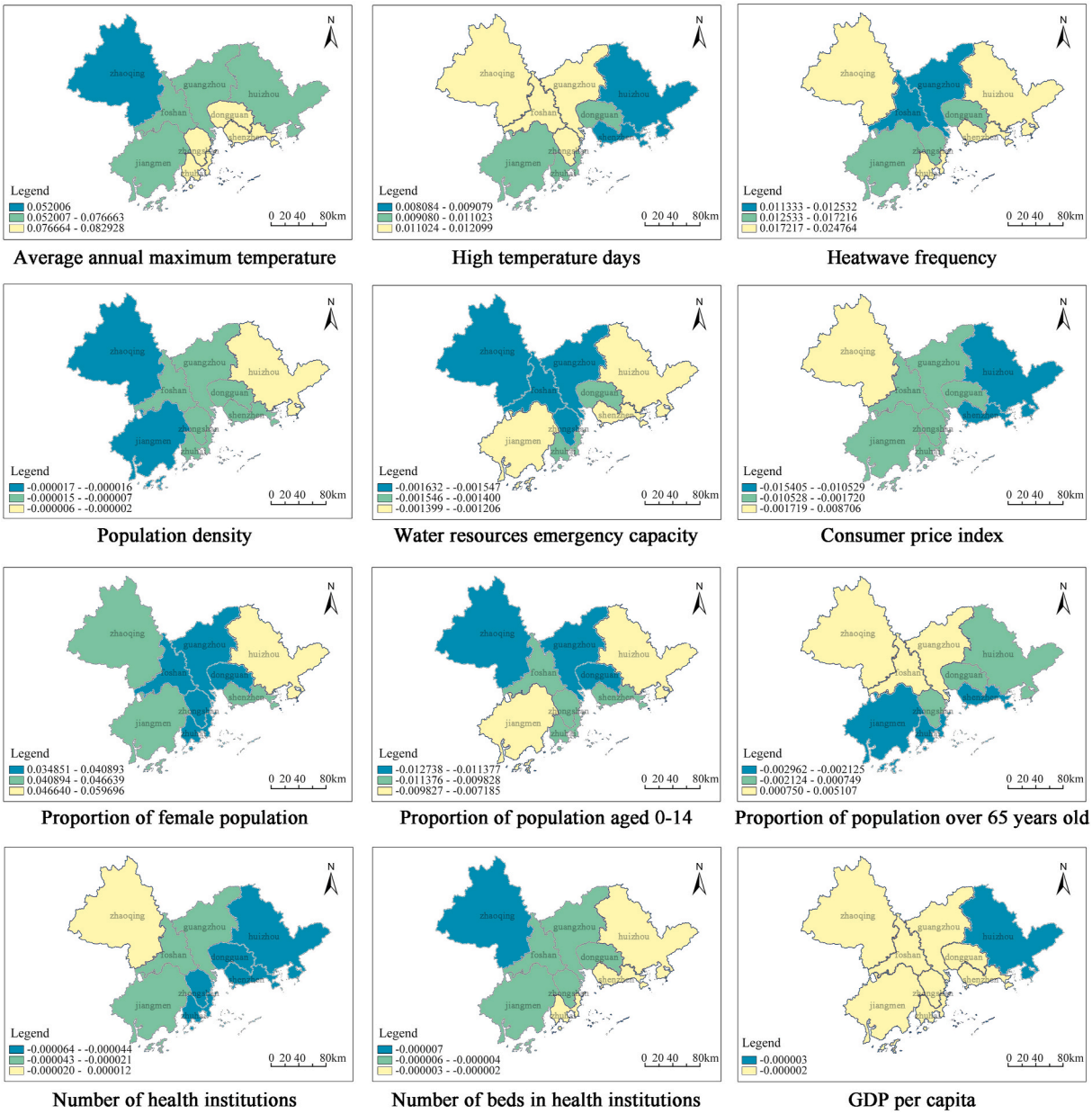

Fig. 7. Map of Regression Coefficients for Influencing Factors on Heat Vulnerability in the study area in 2022.

growth slowed down in 2011, thereby slowing down the change of the HVI. Therefore, in the long run, the growth of population density tends to be an inevitable trend, but with reasonable regulation, its negative impact on heat vulnerability will gradually strengthen. Ensuring that the growth rate of population density is in line with the urbanization process is crucial for decrease the HVI and the exposure to heatwaves.

In the early and late stages of the study, the regression coefficients for water resource emergency capacity showed a small but fluctuating difference, which was determined by the uneven spatial and temporal distribution of water resources in the study area [91]. The mid-term regression coefficients demonstrated a fluctuating downward trend, reflecting the increasing inhibitory effect of controlling the total water resources on the HVI. This was attributed to the water resource management system proposed in the 2011 ″Comprehensive Plan for Water Resources in Guangdong Province [92]". The implementation of the strictest water resource management system in 2013 at the national level has promoted more accurate and systematic planning by local governments for regional water resources [93].

Secondly, the estimated coefficients of CPI showed an overall increasing trend throughout the study period. This indicated that with the development of economic prosperity, residents' purchasing power gradually increases, and their ability to cope with heatwave disasters also improves. The overall regression coefficients gradually approached zero, indicating a weakening inhibitory effect of this indicator. It is necessary for the government and economic research institutions to closely monitor price index data and timely assess changes in residents' living standards.

Thirdly, the fluctuation curves of the female population ratio and the population ratio of 0–14 years old both showed a decreasing trend over time. The proportion of female population in cities was increasing year by year, necessitating special attention to the sensitivity of the female population to heatwaves. Proportion of population aged 0–14 has an inhibitory effect on the change in the HVI. This may be because children aged 0–14 typically have greater physiological adaptability than adults, with a relatively intact temperature regulation system. The implementation of relatively comprehensive social security measures for children in the study area, including education, healthcare, and daily care, alleviates their vulnerability to heatwaves.

Finally, the regression coefficient of proportion of population over 65 years old exhibited a phased change, showing an inhibitory effect from 2011 to 2018. During the period of rapid development in the cities of the study area, the vulnerability assessment may be more influenced by the proportion of the elderly population. More and more studies have confirmed that the elderly are more vulnerable in heatwave disasters [94], sparking high social attention. The study area has introduced policy measures to promote the health and adaptive capacity of the elderly. Therefore, the contribution of the elderly population ratio to the overall vulnerability shifted from positive to negative. From 2019 to 2022, the regression coefficient of the elderly population ratio factor returned to a positive value, possibly due to the gradual strengthening of the aging trend in recent years.

(3) Heat Adaptive Capacity

Adaptation dimension factors had negative regression coefficients, indicating that the number of health institutions, the number of beds in health institutions, and per capita regional GDP all have inhibitory effects on the increase of HVI, with similar effects. Since the 21st century, the rapid development of the study area has improved people's economic standards of living. The construction of urban public health systems has been increasingly perfected, and the continuous stable increase in the construction of health and medical institutions, bed capacity, and staffing of technical personnel has effectively reduced the HVI in the study area.

3.3.3. Spatial heterogeneity of influencing factors

Visualizing the regression coefficients calculated by GTWR on spatial distribution, taking the year 2022 as an example (Fig. 7). In 2022, the high-value areas of heat exposure factor regression coefficients in the study area were mainly located in the northern and eastern regions, showing significant heterogeneity in the primary influencing regions for different factors. The high-value areas of regression coefficients for heat sensitivity factors were mainly in the central region, while the high-value areas for heat adaptive capacity factors were primarily in the surrounding areas.

Overall, the main reasons for the formation of high vulnerability areas in the central and northern parts of the study area were intense and prolonged high-temperature days, frequent heatwave events, and the concentration of high-density populations and economies.

4. Discussion

Based on the conclusions, to further enhance urban resilience to heat risk, this study proposes the following recommendations:

Spatial and temporal differences in thermal vulnerability exist in the study area. The primary concern stems from increasingly severe heat disasters, necessitating enhanced forecasting and warning systems for high temperatures [95]. Currently, China lacks a comprehensive mechanism to address heatwaves. In contrast, the UK established the Heatwave Plan as early as 2014, updated in 2022, which includes a five-level warning service, collaborative response measures across sectors, and systematic monitoring and forecasting. Furthermore, learning from developed countries' experiences, raising public awareness that "heatwaves are disasters" can be beneficial [96]. For instance, the US government created the heat.gov website to visually display national heatwave conditions, aiming to ensure citizen safety and provide tools and resources to combat heatwaves [97]. Taking Zhaoqing as an example, its higher frequency, intensity, and duration of heatwaves compared to other cities highlight the need for targeted monitoring and pilot projects in the Pearl River Delta urban agglomeration.

Moreover, these findings are closely tied to regional economic development, social equity in resource allocation, and

environmental conditions, necessitating attention from relevant authorities. Economically, improving economic development levels is fundamental. Guangzhou and Shenzhen consistently maintain advantages in overall assessments due to their leading economic status. In terms of social equity in resource allocation, disparities in medical facilities and material reserves across regions are evident. This calls for government efforts to strengthen the public health system, ensuring sufficient food, medical services, and health protection during hot weather. Attention should be directed towards vulnerable groups, particularly women and the elderly, by encouraging communities to provide cooling spaces and establish outdoor work standards, as well as using physical cooling methods [98].

Regarding environmental conditions, governments should enhance water resource management, implement water-saving measures, and bolster emergency water reserves to prevent crises at reservoirs during hot weather. Additionally, the study underscores that ongoing improvements in healthcare infrastructure, bed capacity, and skilled personnel effectively reduce heat vulnerability in the study area. Therefore, it is recommended that governments strengthen the construction and support of public health systems to ensure adequate food, medical services, and health protection during high temperatures.

5. Conclusion

In summary, the overall heat vulnerability index (HVI) decreased over time in the study area, with each city showing fluctuating declines and increasing differences among them, especially after 2010. Vulnerable cities like Zhongshan are highly sensitive to heatwaves, underscoring the importance of sharing experiences and resources with nearby less vulnerable areas. Spatially, from 2001 to 2022, heat vulnerability shifted from negative to positive clustering, with noticeable declines in high HVI levels from 2021 to 2022. High-vulnerability cities changed from regional clusters to continuous distributions, indicating significant interdependence and the need to enhance heat adaptation, particularly in cities like Zhaoqing. The GTWR model identified frequent heatwaves, social sensitivity, and changes in residents' consumption as key factors influencing heat vulnerability. Special attention should be given to the frequency and duration of heatwaves, and timely social services for vulnerable groups, especially women and the elderly. Improving economic development, water resources, medical facilities, and promoting green initiatives can establish resilient communities, reduce disaster risks, and support sustainable development planning.

Data availability statement

Data associated with the study has not been deposited into a publicly available repository and the authors do not have permission to share data.

CRediT authorship contribution statement

Jiangbo Wang: Writing – review & editing, Resources, Methodology, Funding acquisition, Formal analysis, Data curation, Conceptualization. **Yishu Li:** Writing – original draft, Supervision, Project administration, Methodology, Data curation, Formal analysis, Funding acquisition, Investigation. **Wei Liu:** Software, Data curation, Supervision. **Aiping Gou:** Writing – review & editing, Conceptualization, Funding acquisition.

Declaration of competing interest

The authors declare that they have no known competing financial interests or personal relationships that could have appeared to influence the work reported in this paper.

Acknowledgments

This research was supported by the National Natural Science Foundation of China, grant number 51978329, 51778364, and the Graduate Research and Innovation Projects of Jiangsu Province, grant number KYCX24_1556.

References

[1] S.E. Perkins, L.V. Alexander, J.R. Nairn, Increasing frequency, intensity and duration of observed global heatwaves and warm spells, Geophys. Res. Lett. 39 (2012), https://doi.org/10.1029/2012gl053361.
[2] X. Huang, Z. Wen, Y. Du, Y. Xu, Scenario analyses on the changes of future surface air temperature and precipitation in south China, J. Trop. Meteorol. (2008) 254–258. https://kns.cnki.net/kcms2/article/abstract?v=uzDkwlsKYf9UZ3ldGmjp0ARqzcqHKKTQH0b7OW-ILnY9FCtNQr-9zOjzhI434cUly7QV2GnqhrjvliPSQ6IuwWlkuJmr7_cNE5Szeq04tkXYw0mC-hkWha4DZaUZffqtHjNc0OiK86I=&uniplatform=NZKPT&language=CHS.
[3] IPCC, Climate change. The Physical Science Basis, 2021, 2021.
[4] U.N.N. Center, WMO: heatwaves and wildfires mark this extreme summer,https://news.un.org/zh/story/2023/07/1120252 (accessed Demcember 20, 2023).
[5] J. Yang, M. Zhou, Z. Ren, M. Li, B. Wang, D.L. Liu, C.-Q. Ou, P. Yin, J. Sun, S. Tong, H. Wang, C. Zhang, J. Wang, Y. Guo, Q. Liu, Projecting heat-related excess mortality under climate change scenarios in China, Nat. Commun. 12 (2021) 1039, https://doi.org/10.1038/s41467-021-21305-1.
[6] A. Le Tertre, A. Lefranc, D. Eilstein, C. Declercq, S. Medina, M. Blanchard, B. Chardon, P. Fabre, L. Filleul, J.F. Jusot, L. Pascal, H. Prouvost, S. Cassadou, M. Ledrans, Impact of the 2003 heatwave on all-cause mortality in 9 French cities, Epidemiology 17 (2006) 75–79, https://doi.org/10.1097/01.ede.0000187650.36636.1f.
[7] K. Knowlton, M. Rotkin-Ellman, G. King, G. Margolis Helene, D. Smith, G. Solomon, R. Trent, P. English, The 2006 California heat wave: impacts on hospitalizations and emergency department visits, Environ. Health Perspect. 117 (2009) 61–67, https://doi.org/10.1289/ehp.11594.

[8] M. Guo, J. Li, J. Xu, X. Wang, H. He, L. Wu, CO2 emissions from the 2010 Russian wildfires using GOSAT data, Environ. Pollut. 226 (2017) 60–68, https://doi.org/10.1016/j.envpol.2017.04.014.

[9] J. Yin, L. Slater, L. Gu, Z. Liao, S. Guo, P. Gentine, Global increases in lethal compound heat stress: hydrological drought hazards under climate change, Geophys. Res. Lett. 49 (2022) e2022GL100880, https://doi.org/10.1029/2022GL100880.

[10] J. Silberner, Heat wave causes hundreds of deaths and hospitalisations in Pacific north west, BMJ Br. Med. J. (Clin. Res. Ed.) 374 (2021), https://doi.org/10.1136/bmj.n1696.

[11] W. Xu, W. Yuan, D. Wu, Y. Zhang, R. Shen, X. Xia, P. Ciais, J. Liu, Impacts of record-breaking compound heatwave and drought events in 2022 China on vegetation growth, Agric. For. Meteorol. 344 (2024) 109799, https://doi.org/10.1016/j.agrformet.2023.109799.

[12] J. Wu, Y. Zhu, Y. Liu, H. Yin, F. Yuan, J. Wang, Spatial-temporal characteristics of heat waves in China, Journal of China Hydrology 42 (2022) 72–77, https://doi.org/10.19797/j.cnki.1000-0852.20210402.

[13] H. Chen, L. Zhao, W. Dong, L. Cheng, W. Cai, J. Yang, J. Bao, X.-Z. Liang, S. Hajat, P. Gong, W. Liang, C. Huang, Spatiotemporal variation of mortality burden attributable to heatwaves in China, 1979-2020, Sci. Bull. 67 (2022) 1340–1344, https://doi.org/10.1016/j.scib.2022.05.006.

[14] C.N.C. Center, China Climate Bulletin in 2022, 2022.

[15] R. Lu, K. Xu, R. Chen, W. Chen, F. Li, C. Lv, Heat waves in summer 2022 and increasing concern regarding heat waves in general, Atmos. Oceanogr. Sci. Libr. 16 (2023) 100290, https://doi.org/10.1016/j.aosl.2022.100290.

[16] D.D. Breshears, J.B. Fontaine, K.X. Ruthrof, J.P. Field, X. Feng, J.R. Burger, D.J. Law, J. Kala, G.E.S.J. Hardy, Underappreciated plant vulnerabilities to heat waves, New Phytol. 231 (2021) 32–39, https://doi.org/10.1111/nph.17348.

[17] J. Wang, Z. Yan, Rapid rises in the magnitude and risk of extreme regional heat wave events in China, Weather Clim. Extrem. 34 (2021) 100379, https://doi.org/10.1016/j.wace.2021.100379.

[18] Y. Liu, H. Jue, W. Zeng, Y. Yang, H. Lin, T. Liu, J. Xiao, X. Li, W. Ma, Y. Ouyang, Short-term effect of heat wave on daily hospital admission in Guangzhou and Xingning, South China Journal of Preventive Medicine 41 (2015) 512–516, https://doi.org/10.13217/j.scjpm.2015.0512.

[19] T.P.s.G.o.G. Province, Notice on issuing the emergency plan for meteorological disasters in Guangdong Province, Gazette of the People's Government of Guangdong Province, 3,https://kns.cnki.net/kcms2/article/abstract?v=uzDkwlsKYf8AoU9rn602eY4-QnFnGCYZaRddQgRSku7Y1pV68sR-GwDI-QoTS3b0vzj2biRCZaUHERS37JgSW4kypl6Cy36jAncNqr_wPiucPms8WcueWITRQP0LFL-zPRIT2Kzzca_BMo2Bzv6f1A==&uniplatform=NZKPT&language=CHS (accessed Demcember 13, 2023).

[20] G.P.D.P.a.R.Y.C. Committee, Guangdong Province Disaster Prevention and Reduction Yearbook, Lingnan Fine Arts Publishing House, Guangzhou, 2012.

[21] J. Zhao, G. He, J. Xiao, G. Zhu, T. Liu, J. Hu, W. Zeng, X. Li, Z. Ren, W. Ma, Mechanism of temperature on dengue fever transmission and impact of future temperature change on its transmission risk, J. Environ. Occup. Med. 39 (2022) 309–314, https://doi.org/10.11836/JEOM21457.

[22] Y. Yue, X. Liu, Y. Guo, N. Zhao, D. Ren, Q. Liu, Spatio-temporal distribution and environmental factors of dengue fever in China, 2020—2022, Journal of Environmental Hygiene 13 (2023) 341–345, https://doi.org/10.13421/j.cnki.hjwsxzz.2023.05.006.

[23] H. Zhang, Y. Pang, X. Zou, T. Zhang, Z. Liao, X. Lin, Y. Qiao, R. Chen, Characteristics of phytoplankton functional groups and their relationships with environmental factors during extreme drought in Xinfengjiang Reservoir, Guangdong Province, J. Lake Sci. (2023) 1–17. https://link.cnki.net/urlid/32.1331.P.20231108.1615.004.

[24] H. Eakin, A.L. Luers, Assessing the vulnerability of social-environmental systems, Annu. Rev. Environ. Resour. 31 (2006) 365–394, https://doi.org/10.1146/annurev.energy.30.050504.144352.

[25] J. Kravchenko, A.P. Abernethy, M. Fawzy, H.K. Lyerly, Minimization of heatwave morbidity and mortality, Am. J. Prev. Med. 44 (2013) 274–282, https://doi.org/10.1016/j.amepre.2012.11.015.

[26] G.A. Meehl, C. Tebaldi, More intense, more frequent, and longer lasting heat waves in the 21st century, Science 305 (2004) 994–997, https://doi.org/10.1126/science.1098704.

[27] C. Aubrecht, D. Ozceylan, Identification of heat risk patterns in the U.S. National Capital Region by integrating heat stress and related vulnerability, Environ. Int. 56 (2013) 65–77, https://doi.org/10.1016/j.envint.2013.03.005.

[28] J. Bao, X. Li, C. Yu, The construction and validation of the heat vulnerability index, a Review, Int. J. Environ. Res. Publ. Health 12 (2015) 7220–7234, https://doi.org/10.3390/ijerph120707220.

[29] M. Christenson, S.D. Geiger, J. Phillips, B. Anderson, G. Losurdo, H.A. Anderson, Heat vulnerability index mapping for Milwaukee and Wisconsin, J. Publ. Health Manag. Pract. : JPHMP 23 (2017) 396–403, https://doi.org/10.1097/phh.0000000000000352.

[30] D.-W. Kim, R.C. Deo, J.-S. Lee, J.-M. Yeom, Mapping heatwave vulnerability in Korea, Nat. Hazards 89 (2017) 35–55, https://doi.org/10.1007/s11069-017-2951-y.

[31] Y. Zhang, X. Huang, D. Zheng, Temporal and spatial characteristics of heat waves and assessment of vulnerability in the Yangtze River Economic Belt, Resour. Environ. Yangtze Basin 32 (2023) 440–450. https://link.cnki.net/urlid/42.1320.X.20221011.0956.002.

[32] Y. Niu, Z. Li, Y. Gao, X. Liu, L. Xu, S. Vardoulakis, Y. Yue, J. Wang, Q. Liu, A systematic review of the development and validation of the heat vulnerability index: major factors, methods, and spatial units, Curr. Clim. Change Rep. 7 (2021) 87–97, https://doi.org/10.1007/s40641-021-00173-3.

[33] M.S.G. Adnan, A. Dewan, D. Botje, S. Shahid, Q.K. Hassan, Vulnerability of Australia to heatwaves: a systematic review on influencing factors, impacts, and mitigation options, Environ. Res. 213 (2022), https://doi.org/10.1016/j.envres.2022.113703.

[34] T. Wolf, W.-C. Chuang, G. McGregor, On the science-policy bridge: do spatial heat vulnerability assessment studies influence policy? Int. J. Environ. Res. Publ. Health 12 (2015) 13321–13349, https://doi.org/10.3390/ijerph121013321.

[35] K. Bradford, L. Abrahams, M. Hegglin, K. Klima, A heat vulnerability index and adaptation solutions for Pittsburgh, Pennsylvania, Environ. Sci. Technol. 49 (2015) 11303–11311, https://doi.org/10.1021/acs.est.5b03127.

[36] T.-L. Chen, H. Lin, Y.-H. Chiu, Heat vulnerability and extreme heat risk at the metropolitan scale: a case study of Taipei metropolitan area, Taiwan, Urban Clim. 41 (2022) 101054, https://doi.org/10.1016/j.uclim.2021.101054.

[37] T. Wolf, G. McGregor, The development of a heat wave vulnerability index for London, United Kingdom, Weather Clim. Extrem. 1 (2013) 59–68, https://doi.org/10.1016/j.wace.2013.07.004.

[38] C.E. Reid, M.S. O'neill, C.J. Gronlund, S.J. Brines, D.G. Brown, A.V. Diez-Roux, J. Schwartz, Mapping community determinants of heat vulnerability, Environ. Health Perspect. 117 (2009) 1730–1736, https://doi.org/10.1289/ehp.0900683.

[39] R. Zhao, X. Li, Y. Wang, Z. Xu, M. Xiong, Q. Jia, F. Li, Assessing resilience of sustainability to climate change in China's cities, Sci. Total Environ. (2023) 898, https://doi.org/10.1016/j.scitotenv.2023.165568.

[40] L. Bai, A. Woodward, Cirendunzhu, Q. Liu, County-level heat vulnerability of urban and rural residents in Tibet, China, Environ. Health 15 (2016), https://doi.org/10.1186/s12940-015-0081-0.

[41] W. Shui, Z. Chen, J. Deng, Y. Li, Q. Wang, W. Wang, Y. Chen, Evaluation of urban high temperature vulnerability of coupling adaptability in Fuzhou, China, Acta Geograph. Sin. 72 (2017) 830–849, https://doi.org/10.11821/dlxb201705006.

[42] C. Wu, W. Shui, Z. Huang, C. Wang, Y. Wu, Y. Wu, C. Xue, Y. Huang, Y. Zhang, D. Zheng, Urban heat vulnerability: a dynamic assessment using multi-source data in coastal metropolis of Southeast China, Front. Public Health 10 (2022), https://doi.org/10.3389/fpubh.2022.989963.

[43] P. Xie, Y. Wang, J. Peng, Y. Liu, Health related urban heat wave vulnerability assessment: research progress and framework, Prog. Geogr. 34 (2015) 165–174. https://link.cnki.net/urlid/11.3858.p.20150212.1424.005.

[44] D.K. Yoon, Assessment of social vulnerability to natural disasters: a comparative study, Nat. Hazards 63 (2012) 823–843, https://doi.org/10.1007/s11069-012-0189-2.

[45] S. Rufat, E. Tate, C.T. Emrich, F. Antolini, How valid are social vulnerability models? Ann. Assoc. Am. Geogr. 109 (2019) 1131–1153, https://doi.org/10.1080/24694452.2018.1535887.

[46] C.-H. Sung, S.-C. Liaw, Using spatial pattern analysis to explore the relationship between vulnerability and resilience to natural hazards, Int. J. Environ. Res. Publ. Health 18 (2021), https://doi.org/10.3390/ijerph18115634.

[47] S.V. Razavi-Termeh, A. Sadeghi-Niaraki, S.-M. Choi, Coronavirus disease vulnerability map using a geographic information system (GIS) from 16 April to 16 May 2020, Phys. Chem. Earth, Parts A/B/C 126 (2022) 103043, https://doi.org/10.1016/j.pce.2021.103043.
[48] S. Jeong, D.K. Yoon, Examining vulnerability factors to natural disasters with a spatial autoregressive model: the case of South Korea, Sustainability 10 (2018) 1651, https://doi.org/10.3390/su10051651.
[49] N. Hu, Z. Zhang, N. Duffield, X. Li, B. Dadashova, D. Wu, S. Yu, X. Ye, D. Han, Z. Zhang, Geographical and temporal weighted regression: examining spatial variations of COVID-19 mortality pattern using mobility and multi-source data, Computational Urban Science 4 (2024) 6, https://doi.org/10.1007/s43762-024-00117-1.
[50] Q. Liu, R. Wu, W. Zhang, W. Li, S. Wang, The varying driving forces of PM2. 5 concentrations in Chinese cities: insights from a geographically and temporally weighted regression model, Environ. Int. 145 (2020) 106168, https://doi.org/10.1016/j.envint.2020.106168.
[51] J.W. Handmer, S. Dovers, T.E. Downing, Societal vulnerability to climate change and variability, Mitig. Adapt. Strategies Glob. Change 4 (1999) 267–281, https://doi.org/10.1023/A:1009611621048.
[52] S. Belliveau, B. Smit, B. Bradshaw, Multiple exposures and dynamic vulnerability: evidence from the grape industry in the Okanagan Valley, Canada, Global Environmental Change-Human and Policy Dimensions 16 (2006) 364–378, https://doi.org/10.1016/j.gloenvcha.2006.03.003.
[53] N.R. Council, Understanding the Changing Planet: Strategic Directions for the Geographical Sciences, National Academies Press, 2010.
[54] S.E. Kershaw, A.A. Millward, A spatio-temporal index for heat vulnerability assessment, Environ. Monit. Assess. 184 (2012) 7329–7342, https://doi.org/10.1007/s10661-011-2502-z.
[55] P. Méndez-Lázaro, F.E. Muller-Karger, D. Otis, M.J. McCarthy, E. Rodríguez, A heat vulnerability index to improve urban public health management in San Juan, Puerto Rico, Int. J. Biometeorol. 62 (2018) 709–722, https://doi.org/10.1007/s00484-017-1319-z.
[56] A.M. Qureshi, A. Rachid, Heat vulnerability index mapping: a case study of a medium-sized city (Amiens), Climate (2022).
[57] S.G. Nayak, S. Shrestha, P.L. Kinney, Z. Ross, S.C. Sheridan, C.I. Pantea, W.H. Hsu, N. Muscatiello, S.A. Hwang, Development of a heat vulnerability index for New York State, Publ. Health 161 (2018) 127–137, https://doi.org/10.1016/j.puhe.2017.09.006.
[58] B. Jalalzadeh Fard, R. Mahmood, M. Hayes, C. Rowe, A.M. Abadi, M. Shulski, S. Medcalf, R. Lookadoo, J.E. Bell, Mapping heat vulnerability index based on different urbanization levels in Nebraska, USA, GeoHealth 5 (2021) e2021GH000478, https://doi.org/10.1029/2021GH000478.
[59] E. Reid Colleen, S. O'Neill Marie, J. Gronlund Carina, J. Brines Shannon, G. Brown Daniel, V. Diez-Roux Ana, J. Schwartz, Mapping community determinants of heat vulnerability, Environ. Health Perspect. 117 (2009) 1730–1736, https://doi.org/10.1289/ehp.0900683.
[60] Q. Zhu, T. Liu, H. Lin, J. Xiao, Y. Luo, W. Zeng, S. Zeng, Y. Wei, C. Chu, S. Baum, Y. Du, W. Ma, The spatial distribution of health vulnerability to heat waves in Guangdong Province, China, Glob. Health Action 7 (2014), https://doi.org/10.3402/gha.v7.25051.
[61] T.G. Frazier, C.M. Thompson, R.J. Dezzani, A framework for the development of the SERV model: a spatially explicit resilience-vulnerability model, Appl. Geogr. 51 (2014) 158–172, https://doi.org/10.1016/j.apgeog.2014.04.004.
[62] B. Huang, B. Wu, M. Barry, Geographically and temporally weighted regression for modeling spatio-temporal variation in house prices, Int. J. Geogr. Inf. Sci. 24 (2010) 383–401, https://doi.org/10.1080/13658810802672469.
[63] N.B.o.S.o. China, Statistical Bulletin of the National Economic and Social Development of the People's Republic of China in 2022, 2022.
[64] Guangdong Statistical Yearbook, Editorial Board and Editing and Publishing Staff, 2023, pp. 4–5.
[65] Y. Zhao, Y. Wang, Y. Xu, Research on the changing characteristics of thermal environment security pattern in the Guangdong-Hong Kong-Macao Greater Bay Area. 2021 China Urban Planning Informatization Annual Conference, 2021, p. 7, https://doi.org/10.26914/c.cnkihy.2021.045123.
[66] M.B.o.G. Province, Climate Monitoring Bulletin of Guangdong-Hong Kong-Macao Greater Bay Area in 2022, 2022.
[67] Y. Lu, Y. Yan, D. Ding, C. Zhao, Y. Song, J. Zhao, Drought trends and their impacts of pressures of urban water resources in China of precipitations, Acta Ecol. Sin. 38 (2018) 1470–1477, https://doi.org/10.5846/stxb201707111248.
[68] J. Li, J. Chen, X. Tang, X. Chen, X. Xu, Analysis of climate change and extreme weather in guangdong-HongKong-Macao greater Bay area, China Flood & Drought Management 31 (2021) 1–6+13, https://doi.org/10.16867/j.issn.1673-9264.2021281.
[69] Z. Huang, H. Chen, H. Tian, Research on the heat wave index, Meteorol. Mon. 37 (2011) 345–351. https://kns.cnki.net/kcms2/article/abstract?v=uzDkwlsKYf8JE7sV05y4SGt3P67lUAn9dS3lbIvq2c1U4_k3Hs4vz9-MKctMk7Njw7ZObHHbxee8sWPtHoj78MsA_7KWOuDEQ34qg_YPVFCtPW4QnQzZ95muWiAGYOWyxgEoVmnOEcw=&uniplatform=NZKPT&language=CHS.
[70] T. Li, P. Niu, C. Gu, A review on research frameworks of resilient cities, Urban Planning Forum (2014) 23–31. https://kns.cnki.net/kcms2/article/abstract?v=uzDkwlsKYf9_6wTnSlzNFt8ukB9y1SIZjMfQspkl8v8JtZ_C5pQgtbBnSrVTlmUqooXHzUsvHYdSqk8hrWh1g9LlOAcjdZs_CuR0H-n77llEppJUPlnLEyD5OdVIPN2Ya2kEZba4bLbBpl9xHTquA==&uniplatform=NZKPT&language=CHS.
[71] W. Suparta, A.N.M. Yatim, An analysis of heat wave trends using heat index in East Malaysia, J. Phys. Conf. 852 (2017) 012005, https://doi.org/10.1088/1742-6596/852/1/012005.
[72] N. Brooks, W. Neil Adger, P. Mick Kelly, The determinants of vulnerability and adaptive capacity at the national level and the implications for adaptation, Global Environ. Change 15 (2005) 151–163, https://doi.org/10.1016/j.gloenvcha.2004.12.006.
[73] J. Schewe, J. Heinke, D. Gerten, I. Haddeland, N.W. Arnell, D.B. Clark, R. Dankers, S. Eisner, B.M. Fekete, F.J. Colón-González, S.N. Gosling, H. Kim, X. Liu, Y. Masaki, F.T. Portmann, Y. Satoh, T. Stacke, Q. Tang, Y. Wada, D. Wisser, T. Albrecht, K. Frieler, F. Piontek, L. Warszawski, P. Kabat, Multimodel assessment of water scarcity under climate change, Proc. Natl. Acad. Sci. USA 111 (2014) 3245–3250, https://doi.org/10.1073/pnas.1222460110.
[74] G. Hatvani-Kovacs, M. Belusko, N. Skinner, J. Pockett, J. Boland, Heat stress risk and resilience in the urban environment, Sustain. Cities Soc. 26 (2016) 278–288, https://doi.org/10.1016/j.scs.2016.06.019.
[75] M. Stafoggia, F. Forastiere, D. Agostini, A. Biggeri, L. Bisanti, E. Cadum, N. Caranci, F. de'Donato, S. De Lisio, M. De Maria, P. Michelozzi, R. Miglio, P. Pandolfi, S. Picciotto, M. Rognoni, A. Russo, C. Scarnato, C.A. Perucci, Vulnerability to heat-related mortality: a multicity, population-based, case-crossover analysis, Epidemiology 17 (2006), https://doi.org/10.1097/01.ede.0000208477.36665.34.
[76] Z. Xu, P.E. Sheffield, H. Su, X. Wang, Y. Bi, S. Tong, The impact of heat waves on children's health: a systematic review, Int. J. Biometeorol. 58 (2014) 239–247, https://doi.org/10.1007/s00484-013-0655-x.
[77] J. Garssen, C. Harmsen, J. De Beer, The effect of the summer 2003 heat wave on mortality in The Netherlands, Euro Surveill. 10 (2005) 13–14, https://doi.org/10.2807/esm.10.07.00557-en.
[78] C.K. Uejio, O.V. Wilhelmi, J.S. Golden, D.M. Mills, S.P. Gulino, J.P. Samenow, Intra-urban societal vulnerability to extreme heat: the role of heat exposure and the built environment, socioeconomics, and neighborhood stability, Health Place 17 (2011) 498–507, https://doi.org/10.1016/j.healthplace.2010.12.005.
[79] X. Luo, Y. Du, J. Zheng, Risk regionalization of human health caused by high temperature & heat wave in Guangdong Province, Climate Change Research 12 (2016) 139–146, https://doi.org/10.12006/j.issn.1673-1719.2015.155.
[80] Y. Linchuan, Y. Haosen, F. Qiangxue, Z. Guilin, Y. Bingjie, Vulnerability assessment and planning response to high-temperature wave in large cities: the case of Chengdu, Planner 39 (2023) 38–45. https://kns.cnki.net/kcms2/article/abstract?v=_Kb8wOrUs9vGexlwtYXejllRjr80jrF2MKufF0ODGmiNph4nOMU_cTiyfnprV-CPZe5dMEesH9Pri3oMmBtR8OzepmMRFDrQEbUV3Z1otdV9WBu7Pjvtz4_rAt8_ij9PWMKA01gB12Kv5XBMx-Wyg==&uniplatform=NZKPT&language=CHS.
[81] S.L. Cutter, B. Boruff, W.L. Shirley, Social vulnerability to environmental hazards, Soc. Sci. Q. 84 (2003) 242–261, https://doi.org/10.1111/1540-6237.8402002.
[82] K.P. Gallo, A.L. McNab, T.R. Karl, J.F. Brown, J.J. Hood, J.D. Tarpley, The use of a vegetation index for assessment of the urban heat island effect, Int. J. Rem. Sens. 14 (1993) 2223–2230, https://doi.org/10.1080/01431169308954031.
[83] J. Zhao, G. Ji, Y. Tian, Y. Chen, Z. Wang, Environmental vulnerability assessment for mainland China based on entropy method, Ecol. Indicat. 91 (2018) 410–422, https://doi.org/10.1016/j.ecolind.2018.04.016.
[84] X. Li, Y. Wang, S. Zheng, Y. Huang, Resilience measurement and spatial and temporal dynamic evolution analysis of rural infrastructure in the Yangtze River Economic Belt, Stat. Decis. 39 (2023) 79–84, https://doi.org/10.13546/j.cnki.tjyjc.2023.12.014.

[85] W. Wang, X. Yu, P. Yang, D. Ma, Spatial and temporal patterns of disaster resilience and spatial convergence in the Beijing-Tianjin-Hebei City Cluster, Journal of Catastrophology 38 (2023) 1–6, https://doi.org/10.3969/j.issn.1000-811X.2023.04.001.
[86] L. Anselin, Local indicators of spatial association—lisa, Geogr. Anal. 27 (1995) 93–115, https://doi.org/10.1111/j.1538-4632.1995.tb00338.x.
[87] P. Tian, J. Li, L. Wang, R. Liu, X. Shi, Dynamics of three-dimensional ecological footprint of Zhejiang coastal zone and its influencing factors based on GTWR model, Chin. J. Appl. Ecol. 31 (2020) 3173–3186, https://doi.org/10.13287/j.1001-9332.202009.016.
[88] H. Wang, B. Zhang, Y. Liu, Y. Liu, S. Xu, Y. Deng, Y. Zhao, Y. Chen, S. Hong, Multi-dimensional analysis of urban expansion patterns and their driving forces based on the center of gravity-GTWR model: a case study of the Beijing-Tianjin-Hebei urban agglomeration, Acta Geograph. Sin. 73 (2018) 1076–1092, https://doi.org/10.11821/dlxb201806007.
[89] X. Chen, W. Pan, J. Zhang, X. Luo, Significant warming increases extreme weather events in Guangzhou, Guangdong Meteorology (2007) 24–25. https://kns.cnki.net/kcms2/article/abstract?v=uzDkwlsKYf8pqT3GjJlL1kxgQJE-sFXB2d9dHMD438pVsjF6zBzwFOJqE6eEDnY6bBr2KgJWg13zkDVd9nA4hNqNgT0Hg-rz9rSgbIRxlIAf8EVtn5xOBnJk6WvTwFDSNEAWWyQO3HA=&uniplatform=NZKPT&language=CHS.
[90] J.D.H.B.o.J. City, Interpretation of health cooperation and development in the outline development plan for the Guangdong-Hong Kong-Macao Greater Bay Area. http://www.jianghai.gov.cn/bwbj/wsjkj/zwdt/content/post_1125631.html, 2019. Demcember 1, 2023.
[91] T.P.s.G.o.G. Province, A multi-pronged approach is taken to build a new pattern of spatiotemporal distribution of water resources, and the uneven spatiotemporal distribution of water resources in Guangdong is expected to be improved. https://www.gd.gov.cn/gdywdt/bmdt/content/post_3246492.html, 2021. (Accessed 10 January 2024).
[92] T.P.s.G.o.G. Province, Approval of the Comprehensive Water Resources Planning of Guangdong Province, 2011. https://www.gd.gov.cn/gkmlpt/content/0/140/post_140044.html#7. (Accessed 10 January 2024).
[93] Q. Zuo, D. Hu, M. Dou, X. Zhang, J. Ma, Framework and core system of the most stringent water resource management system based on the concept of human-water harmony, Resour. Sci. 36 (2014) 906–912. https://kns.cnki.net/kcms2/article/abstract?v=r-3vL8vLwqkYwyCAE7wnZ45lEpE1uwy02ms3DKwDYEIY7KYSOR58MEARASOw9V61SeCFn31xtybovc16yvxZ7RZB7u9rs-2WvfMCGyunfC2xAoOy0LBnEYihSWfxRtS61AJPtBSmY9k=&uniplatform=NZKPT&language=CHS.
[94] R.D. Meade, A.P. Akerman, S.R. Notley, R. McGinn, P. Poirier, P. Gosselin, G.P. Kenny, Physiological factors characterizing heat-vulnerable older adults: a narrative review, Environ. Int. 144 (2020) 105909, https://doi.org/10.1016/j.envint.2020.105909.
[95] B. He, M. Yin, Global actions, strategies and guidelines for beating urban heat, Urban Planning International, 1-16, https://doi.org/10.19830/j.upi.2022.340.
[96] T. Liu, Y.J. Xu, Y.H. Zhang, Q.H. Yan, X.L. Song, H.Y. Xie, Y. Luo, S. Rutherford, C. Chu, H.L. Lin, W.J. Ma, Associations between risk perception, spontaneous adaptation behavior to heat waves and heatstroke in Guangdong province, China, BMC Publ. Health 13 (2013), https://doi.org/10.1186/1471-2458-13-913.
[97] K. Vanderplanken, J. van Loenhout, Y. Inaç, D. Guha-Sapir, Critical Analysis of Heat Plans and Interviews, SCORCH project, 2020.
[98] O. Jay, A. Capon, P. Berry, C. Broderick, R. de Dear, G. Havenith, Y. Honda, R.S. Kovats, W. Ma, A. Malik, N.B. Morris, L. Nybo, S.I. Seneviratne, J. Vanos, K. L. Ebi, Reducing the health effects of hot weather and heat extremes: from personal cooling strategies to green cities, Lancet 398 (2021) 709–724, https://doi.org/10.1016/S0140-6736(21)01209-5.